

## Methotrexate Loaded Polyether-Copolyester Dendrimers for the Treatment of Gliomas: Enhanced Efficacy and Intratumoral Transport Capability

Renu Singh Dhanikula,<sup>†</sup> Anteneh Argaw,<sup>‡</sup> Jean-Francois Bouchard,<sup>‡</sup> and Patrice Hildgen<sup>\*†</sup>

Faculty of Pharmacy, Pavillon Jean-Coutu, and School of Optometry, University of Montreal, C.P. 6128, Succursale Centre-ville, Montreal, Quebec, Canada H3C 3J7

Received June 27, 2007; Revised Manuscript Received October 1, 2007; Accepted October 2, 2007

**Abstract:** Therapeutic benefit in glial tumors is often limited due to low permeability of delivery systems across the blood–brain barrier (BBB), drug resistance, and poor penetration into the tumor tissue. In an attempt to overcome these hurdles, polyether-copolyester (PEPE) dendrimers were evaluated as drug carriers for the treatment of gliomas. Dendrimers were conjugated to D-glucosamine as the ligand for enhancing BBB permeability and tumor targeting. The efficacy of methotrexate (MTX)-loaded dendrimers was established against U87 MG and U 343 MGa cells. Permeability of rhodamine-labeled dendrimers and MTX-loaded dendrimers across the *in vitro* BBB model and their distribution into avascular human glioma tumor spheroids was also studied. Glucosylated dendrimers were found to be endocytosed in significantly higher amounts than nonglucosylated dendrimers by both the cell lines. IC<sub>50</sub> of MTX after loading in dendrimers was lower than that of the free MTX, suggesting that loading MTX in PEPE dendrimers increased its potency. Similar higher activity of MTX-loaded glucosylated and nonglucosylated dendrimers was found in the reduction of tumor spheroid size. These MTX-loaded dendrimers were able to kill even MTX-resistant cells highlighting their ability to overcome MTX resistance. In addition, the amount of MTX-transported across BBB was three to five times more after loading in the dendrimers. Glucosylation further increased the cumulative permeation of dendrimers across BBB and hence increased the amount of MTX available across it. Glucosylated dendrimers distributed through out the avascular tumor spheroids within 6 h, while nonglucosylated dendrimers could do so in 12 h. The results show that glucosamine can be used as an effective ligand not only for targeting glial tumors but also for enhanced permeability across BBB. Thus, glucosylated PEPE dendrimers can serve as potential delivery system for the treatment of gliomas.

**Keywords:** Dendrimer; gliomas; tumor spheroids; methotrexate

### 1. Introduction

Though not highly prevalent, brain tumors are one of the most lethal forms of cancer. They are the leading cause of

solid tumor death in children under age of 20 and are the third leading cause of cancer death in young adults ages 20–39 years.<sup>1</sup> In the year 2000, approximately 176 000 new cases of brain and other central nervous system (CNS) tumors were diagnosed worldwide, with an estimated mortality of 128 000.<sup>2</sup> It is reported that only 5% of patients survive from

\* To whom correspondence should be addressed. Mailing address: Faculty of Pharmacy, Pavillon Jean-Coutu, C.P. 6128, Succursale Centre-ville, Montreal, Quebec, Canada H3C 3J7. Tel: 514-343-6448. Fax: 514-343-2102. Email: patrice.hildgen@umontreal.ca.

<sup>†</sup> Faculty of Pharmacy.

<sup>‡</sup> School of Optometry.

(1) Landis, S.; Murray, T.; Bolden, S.; Wingo, P. Cancer statistics, 1999. *Cancer J. Clinicians* **1999**, *49*, 8–31.

(2) Parkin, D.; Bray, F.; Ferlay, J.; Pisani, P. Estimating the world cancer burden: Globocan 2000. *Int. J. Cancer* **2001**, *94*, 153–156.

brain tumors after 5 years of diagnosis. In fact, the patients with brain tumors have poorer survival rates than breast cancer patients. Most of the systemically administered chemotherapeutic agents do not enter the brain in adequate amounts. Consequently, high doses of drugs are administered systemically to obtain required brain tumor concentration, causing systemic toxicity and thereby compromising the quality of patient life. Due to these limitations of the conventional delivery methods, brain tumors remain an unsolved clinical problem in spite of decades of research. Thus, there is a need for multifunctional carrier that can be engineered into a single nanoplatform such that it can carry drug, cross the blood–brain barrier (BBB), and target the tumors. In this direction, dendrimers can serve as a versatile targeting platform due to their unique structural and functional advantages instigating from the multiple surface groups that can be used for conjugating multifunctional ligands<sup>3,4</sup> and from the presence of internal voids in which drugs can be easily encapsulated or complexed.<sup>5,6</sup> These interior voids provide a nanocompartment in the dendrimers where the loaded drug is protected from the external environment. Further, dendrimers have a small nanometric size which can provide the additional advantage of increased permeability across the barriers.

Receptor-mediated endocytosis is one of the major mechanism by which various agents can traverse the BBB. The receptors for insulin, transferrin, endothelial growth factors, amino acids, and various metabolic nutrients are expressed on BBB.<sup>7</sup> Glucose transporter GLUT-1 is one such transporter found in high density on BBB.<sup>8,9</sup> Glucose transporters such as GLUT-1 are also known to be overexpressed on the tumors of brain, colon, liver, lung, pancreas, stomach, and

retina.<sup>10–12</sup> Targeting to various tumors by the glucose transporters has been successfully done for positron emission tomography,<sup>13,14</sup> magnetic resonance contrast imaging,<sup>11</sup> and gene targeting.<sup>15</sup> Glucose conjugation to the delivery system confers tumor-targeting property through facilitative glucose metabolism by the glucose transporters in the tumors.<sup>16</sup> Thus, glucose can be used not only for enhanced delivery across the BBB but also for targeting to the brain tumors. Considering the advantage of dual targeting using the same ligand and synthetic simplicity of conjugating a single ligand, glucose was used as a targeting moiety in the present work.

Most of the brain tumors are solid tumors. Recently, it has been suggested that limited penetration of drugs in solid tumors is one of the causes of poor therapeutics indices of many chemotherapeutic agents.<sup>17</sup> In particular, the avascular regions of solid tumors represent a major obstacle in achieving the effective control of the tumor growth.<sup>18</sup> In many solid tumors, the cellular population could be more than 100  $\mu\text{m}$  apart from the vasculature; as a consequence, the drug and nutrient distribution to the distant cells is limited. In addition to the limited vasculature, high cell density, elevated interstitial pressure, hypoxia, and acidic

- (3) Aulenta, F.; Hayes, W.; Rannard, S. Dendrimers: a new class of nanoscopic containers and delivery devices. *Eur. Polym. J.* **2003**, *39*, 1741–1771.
- (4) Klajnert, B.; Bryszewska, M. Dendrimers: properties and applications. *Acta Biochim. Pol.* **2001**, *48*, 199–208.
- (5) Esfand, R.; Tomalia, D. A. Poly(amidoamine) (PAMAM) dendrimers: from biomimicry to drug delivery and biomedical applications. *Drug Discovery Today* **2001**, *6*, 427–436.
- (6) Patri, A. K.; Majoros, I. J.; Baker, J. R. Dendritic polymer macromolecular carriers for drug delivery. *Current Opin. Chem. Biol.* **2002**, *6*, 466–471.
- (7) Smith, M. W.; Gumbleton, M. Endocytosis at the blood-brain barrier: from basic understanding to drug delivery strategies. *J. Drug Target.* **2006**, *14*, 191–214.
- (8) McAllister, M. S.; Krizanac-Bengez, L.; Macchia, F.; Naftalin, R. J.; Pedley, K. C.; Mayberg, M. R.; Marroni, M.; Leaman, S.; Stanness, K. A.; Janigro, D. Mechanisms of glucose transport at the blood-brain barrier: an in vitro study. *Brain Res.* **2001**, *409*, 20–30.
- (9) Partridge, W.; Boado, R.; Farrell, C. Brain-type glucose transporter (GLUT-1) is selectively localized to the blood-brain barrier. Studies with quantitative western blotting and in situ hybridization. *J. Biol. Chem.* **1990**, *265*, 18035–18040.

- (10) Airley, R.; Loncaster, J.; Davidson, S.; Bromley, M.; Roberts, S.; Patterson, A.; Hunter, R.; Stratford, I.; West, C. Glucose transporter Glut-1 expression correlates with tumor hypoxia and predicts metastasis-free survival in advanced carcinoma of the cervix. *Clin. Cancer Res.* **2001**, *7*, 928–934.
- (11) Luciani, A.; Olivier, J.-C.; Clement, O.; Siauve, N.; Brillet, P.-Y.; Bessoud, B.; Gazeau, F.; Uchebgu, L. F.; Kahn, E.; Fria, G.; Cuenod, C. A. Glucose-receptor MR imaging of tumors: Study in mice with PEGylated paramagnetic niosomes. *Radiology* **2004**, *231*, 135–142.
- (12) Pedersen, P. L.; Mathupala, S.; Rempel, A.; Geschwind, J.; Ko, Y. H. Mitochondrial bound type II hexokinase: a key player in the growth and survival of many cancers and an ideal prospect for therapeutic intervention. *Biochim. Biophys. Acta* **2002**, *1555*, 14–20.
- (13) Haberkorn, U.; Ziegler, S.; Oberdorfer, F.; Trojan, H.; Haag, D.; Peschke, P.; Berger, M.; Altmann, A.; Kaick, G. v. FDG uptake, tumor proliferation and expression of glycolysis associated genes in animal tumor models. *Nucl. Med. Biol.* **1994**, *21*, 827–834.
- (14) Maublant, J.; Vuillez, J.; Talbot, J.; Lumbroso, J.; Muratet, J.; Herry, J.; Artus, J. Positron emission tomography (PET) and (F-18)-fluorodeoxyglucose in (FDG) in cancerology. *Bull. Cancer* **1998**, *85*, 935–950.
- (15) Park, I.; Cook, S.; Kim, Y.; Kim, H.; Cho, M.; Jeong, H.; Kim, E.; Nah, J.; Bom, H.; Cho, C. Glucosylated polyethylenimine as a tumor-targeting gene carrier. *Arch. Pharm. Res.* **2005**, *28*, 1302–1310.
- (16) Noguchi, Y.; Saito, A.; Miyagi, Y.; Yamanaka, S.; Marat, D.; Doi, C.; Yoshikawa, T.; Tsuburaya, A.; Ito, T.; Satoh, S. Suppression of facilitative glucose transporter 1 mRNA can suppress tumor growth. *Cancer Lett.* **2000**, *154*, 175–182.
- (17) Minchinton, A.; Tannock, I. Drug penetration in solid tumours. *Nat. Rev. Cancer* **2006**, *6*, 583–592.
- (18) Kostarelos, K.; Emfietzoglou, D.; Papakostas, A.; Yang, W. H.; Ballangrud, A. M.; Sgouros, G. Engineering lipid vesicles of enhanced intratumoral transport capabilities: correlating liposome characteristics with penetration into human prostate tumor spheroids. *J. Liposome Res.* **2005**, *15*, 15–27.

pH<sup>19</sup> impede the penetration, distribution, and cellular accumulation of chemotherapeutic agents in these distant tumor cells.<sup>20</sup> For a treatment to be effective, it should access the entire tumor, since survival of even a few cells could result in cancer recurrence. Indeed, the poor therapeutic indices of delivery systems like liposomes due to poor diffusion/penetration within the interstitial space of tumors have been repeatedly documented in the literature.<sup>21,22</sup> Thus, distribution of drug in avascular regions of the tumor is one of the most challenging tasks. For these reasons, preliminary evaluation of interaction and diffusion of delivery systems within an avascular tumor model can serve as an extremely valuable tool for optimizing delivery systems for anticancer therapeutics.<sup>18</sup> Tumor spheroids display a three-dimensional representation of avascular regions found in many solid tumor tissues.<sup>23,24</sup> They have extensive cell–cell contact, elevated interstitial pressure, hypoxia, presence of quiescent cells, and gradient of nutrient concentration and cellular proliferation from the exterior to the center.<sup>20,25</sup> Therefore, they can serve as invaluable tool for this purpose.

The objective of this study was to determine the potential of polyether-copolyester (PEPE) dendrimers loaded with methotrexate (MTX) in the treatment of gliomas. PEPE dendrimers were conjugated to D-glucosamine for enhanced delivery across the BBB as well as for targeting the tumors. The tumoricidal activity of these MTX loaded dendrimers was evaluated against glioma cells and the avascular human glioma tumor spheroids. The ability of fluorescently labeled dendrimers to penetrate within the tumor spheroids was investigated using confocal laser scanning microscopy.

## 2. Experimental Section

**2.1. Materials.** D-Glucosamine, disuccinimidyl carbonate, rhodamine-B, fluorescein isothiocyanate (FITC), 4-(dimethyl-

- (19) Brown, J. M.; Giaccia, A. J. The unique physiology of solid tumors: opportunities (and problems) for cancer therapy. *Cancer Res.* **1998**, *58*, 1408–1416.
- (20) Kostarelos, K.; Emfietzoglou, D.; Papakostas, A.; Yang, W. H.; Ballangrud, A.; Sgouros, G. Binding and interstitial penetration of liposomes within avascular tumor spheroids. *Int. J. Cancer* **2004**, *112*, 713–721.
- (21) Ishida, O.; Maruyama, K.; Sasaki, K.; Iwatsuru, M. Size-dependent extravasation and interstitial localization of polyethyleneglycol liposomes in solid tumor-bearing mice. *Int. J. Pharm.* **1999**, *190*, 49–56.
- (22) Yuan, F.; Leunig, M.; Huang, S.; Berk, D.; Papahadjopoulos, D.; Jain, R. Microvascular permeability and interstitial penetration of sterically stabilized (stealth) liposomes in a human tumor xenograft. *Cancer Res.* **1994**, *54*, 3352–3356.
- (23) Mellor, H. R.; Davies, L. A.; Caspar, H.; Pringle, C. R.; Hyde, S. C.; Gill, D. R.; Callaghan, R. Optimising non-viral gene delivery in a tumour spheroid model. *J. Gene Med.* **2006**, *8*, 1160–1170.
- (24) Mellor, H. R.; Ferguson, D. J.; Callaghan, R. A model of quiescent tumour microregions for evaluating multicellular resistance to chemotherapeutic drugs. *Br. J. Cancer* **2005**, *93*, 302–309.
- (25) Desoize, B.; Jardillier, J. Multicellular resistance: a paradigm for clinical resistance? *Crit. Rev. Oncol. Hematol.* **2000**, *36*, 193–207.

**Table 1.** Hydrodynamic Size and MTX Loading in Dendrimers

dendrimer	hydrodynamic size (nm) <sup>a</sup>	drug loading (w/w) <sup>b</sup>	encapsulation efficiency (%) <sup>c</sup>
Den-1-(G2)-200	3.58 (0.11)	17.2 ± 1.8	62.8 ± 8.4
Den-1-(G2)-300	4.74 (0.13)	19.1 ± 1.1	65.5 ± 6.5
Den-1-(G2)-400	5.41 (0.27)	21.9 ± 1.7	71.9 ± 8.2
Den-1-(G2)-400-Glu	7.52 (0.34)	19.4 ± 1.3	64.0 ± 8.5
Den-2-(G2)-200	4.19 (0.11)	20.3 ± 1.0	68.8 ± 6.3
Den-2-(G2)-300	4.83 (0.19)	22.9 ± 1.2	73.3 ± 6.9
Den-2-(G2)-400	7.41 (0.14)	24.5 ± 1.1	78.4 ± 6.6
Den-2-(G2)-400-Glu	11.24 (0.41)	20.8 ± 1.5	67.3 ± 7.1

<sup>a</sup> Data are mean (PI) ( $n = 5$ ). <sup>b</sup> Where w/w stands for weight of MTX (mg) loaded per unit weight of dendrimer (mg); data are mean ± SD ( $n = 4–6$ ). <sup>c</sup> Where encapsulation efficiency defines percent of the ratio of MTX loaded in the dendrimers to that added initially; data are mean ± SD ( $n = 4–6$ ).

lamino)pyridine, 1-ethyl-3-[3-(dimethylamino)propyl]carbodiimide hydrochloride (EDC), Triton-X 100, poly-D-lysine (MW 196 400), 3-(4,5-dimethylthiazol-2-yl)-2,5-diphenyltetrazolium bromide (MTT), MTT solubilization solution, ethidium bromide, and dihydrofolate reductase assay kit were purchased from Sigma Chemical Co. (Oakville, ON). *N,N*-Dimethylformamide (DMF) and paraformaldehyde were supplied by Aldrich Chemicals, Inc. (Oakville, ON). Dialysis tubing (MWCO 3500 and 6000–8000 Da) was obtained from Fisher Scientific Co. (Ottawa, ON). The bicinchonic acid (BCA) protein assay kit used to characterize protein levels was obtained from Pierce Biotechnology (Rockford, IL). MTX was purchased from Toronto Research Chemicals, Inc. (North York, ON). Dulbecco's modified Eagle's medium (DMEM), Hanks' balanced salt solution (HBSS), nonessential amino acids, fetal bovine serum (FBS), and antibiotics were purchased from Invitrogen Canada (Burlington, ON). All other chemicals and solvents were of reagent grade and were used without purification unless specified otherwise.

**2.2. Methods. 2.2.1. Dendrimers Evaluated.** Two series of PEPE dendrimers, namely den-1-series and den-2-series, were evaluated in this study (Table 1). Here, the dendrimers are referred to as den-1-(Gn)-M or den-2-(Gn)-M, where 1 and 2 represent dendrimers containing dihydroxy benzoic acid (DHBA) and gallic acid, respectively; Gn represents the generation and M denotes the molecular weight of polyethylene oxide (PEO) used in the interior cavity of the dendrimers. The synthetic scheme utilized for the synthesis of PEPE dendrimers is included in the Supporting Information (Scheme 1s and 2s); however, the detailed synthesis and chemical characterization is reported elsewhere.<sup>26,27</sup>

**2.2.2. Conjugation of Glucosamine to the Dendrimers.** D-Glucosamine (4.5 mM) was dissolved in dry acetone; later, disuccinimidyl carbonate (0.54 mM) and dimethyl aminopy-

- (26) Dhanikula, R.; Hildgen, P. Synthesis and evaluation of novel dendrimers with hydrophilic interior as nanocarriers for drug delivery. *Bioconjugate Chem.* **2006**, *17*, 29–41.
- (27) Dhanikula, R.; Hildgen, P. Influence of molecular architecture of polyether-co-polyester dendrimers on the encapsulation and release of methotrexate. *Biomaterials* **2007**, *28*, 3140–3152.

ridine (2.3 mM) were added, and the reaction was allowed to continue for 48 h. Acetone was evaporated on a rotatory evaporator, and the product was dissolved in methanol and purified by extraction with ether (three times) and chloroform (three times). Subsequently, methanol was evaporated and product was dried under vacuum. The allyl pendant terminal groups of dendrimers were oxidized to hydroxyl groups as reported previously.<sup>26</sup> The succinimidyl carbonate derivative of glucosamine (2.7  $\mu$ M) was then conjugated to these hydroxyl dendrimers (2.7  $\mu$ M) by incubating them in dry acetone and DMF (10:1) at room temperature for 96 h. Product was purified by dialysis against water for 96 h using a dialysis membrane of MWCO 6000–8000 Da. Conjugation of glucosamine to dendrimers was determined by <sup>1</sup>HNMR.

**2.2.3. Fluorescent Labeling of the Dendrimers.** The conjugation of rhodamine B to the dendrimers was carried out as reported previously.<sup>28</sup> In the case of den-1-(G2)-400, pendant allyl terminal functional groups were oxidized to hydroxyl groups<sup>26</sup> to obtain the hydroxyl derivative of the dendrimers. Later, hydroxyl derivatives of den-1-(G2)-400 or glucosamine conjugates of den-1-(G2)-400 (den-1-(G2)-400-Glu) were dissolved in DMF. EDC (0.1 mM), DMAP (0.08 mM), and rhodamine B (0.08 mM) were added to the flask and the reaction was allowed to occur for 48 h. Precipitate of EDC-urea was removed by filtration and product was purified by dialysis (MWCO 6000–8000 Da) against deionized water for 96 h. *In vitro* stability of rhodamine-dendrimer conjugates was assessed in PBS (pH 7.4) at 37 °C. No dissociation of rhodamine from dendrimers was observed for 3 days, indicating a stable linkage.

**2.2.4. MTX Encapsulation.** Dendrimers were dissolved in DMF in screw-capped vials, MTX was added to these vials and samples were stirred at room temperature for 48 h. Unencapsulated drug was removed by dialysis (MWCO 3500 Da) for 4 h against 4 L of deionized water. The dialysate was lyophilized to obtain freeze-dried dendrimer loaded with MTX. Drug loading was determined by adding freeze-dried dendrimers to DMF, sonicating them (550 Sonic dismembrator, Fisher Scientific, Ottawa, ON) for 1 min, and later agitating for 24 h at 200 rpm. MTX was analyzed using UV spectrophotometer U-2001 (Hitachi high technologies, Orlando, FL) at 376 nm with appropriate blank corrections.

**2.2.5. Internalization of Dendrimers by Glioma Cells.** U 87 MG and U 343 MGa cells (kind gift from J.-F. Bouchard, University of Montreal) ((American type Culture Collection (ATCC), Rockville, MD) (passage 15–20) were seeded at a concentration of  $1 \times 10^5$  cells/mL (300  $\mu$ L/well) into 24-well cell culture plates and were allowed to adhere to the wells for 24 h. Rhodamine-labeled dendrimers (100  $\mu$ g/mL, in HBSS) were added to each well and incubated for 4 h at 37 °C. Subsequently, cells were washed four times with HBSS to remove dendrimer adhering to the cellular surface. Cells were then lysed with 200  $\mu$ L of 0.5% Triton-X

containing 0.1 N NaOH. Dendrimer concentrations in the cell lysate was determined by measuring rhodamine fluorescence ( $\lambda_{\text{ex}}$  550 nm and  $\lambda_{\text{em}}$  625 nm) using Safire plate reader (Tecan Austria GmbH, Salzburg, Austria). Standard curve generated using lysed cells and rhodamine-labeled dendrimers was used for the quantification of fluorescence. Protein content of each well was estimated by using micro BCA protein assay reagent.

**2.2.6. Intracellular Localization of Dendrimers.** U 343 MGa cells (passage 15–20) were plated at the density of  $0.5 \times 10^6$  cells/mL on glass coverslips treated with 0.05% w/v of poly-D-lysine solution. Cells were allowed to grow to 80% confluence. Later, rhodamine-labeled dendrimers (200  $\mu$ g/mL) were added to each well and incubated for 4 h. After incubation, slides were washed four times with HBSS, fixed with formaldehyde (1% w/v in PBS) for 30 min, and again washed with HBSS two times. Coverslips were then mounted on slides using GelTol mounting medium (Thermo Electron Corp., PA). Confocal laser scanning microscope images were acquired at 100 $\times$  using DMRXE microscope (Zeiss, Oberkochen, Germany) equipped with Leica TCS SP 2 confocal system (Leica Microsystems, Heidelberg, Germany).

**2.2.7. Development of MTX-Resistant U 87 MG Cells.** U 87 MG cells were grown in DMEM supplemented with 10% FBS, 1% nonessential amino acids, penicillin/streptomycin and 500 nM of MTX at 37 °C in a 5% CO<sub>2</sub> atmosphere. The production of MTX resistance in cells was followed by observing the size of the cells and nuclei, MTX-FITC accumulation in the cells, and dihydrofolate reductase activity.

**(a) Enzyme Assay.** Activity of dihydrofolate in the glioma cells was determined by preparing cell extracts as described previously by Alt et al.<sup>29</sup> Cells were harvested from monolayer by trypsinization, washed three times with HBSS, and suspended in ice-cold 50 mM potassium phosphate (pH 7.0). This suspension was disrupted with a probe sonicator for 5 min. Later, it was centrifuged at 100000g for 60 min at 4 °C to yield supernatant called cell extract. Folate reductase activity in the cell extract was determined using dihydrofolate reductase assay kit. Protein content of the cell extract was determined by BCATM protein assay kit.

**(b) MTX-FITC Accumulation.** MTX was conjugated with FITC according to the procedure mentioned by Gapski et al.<sup>30</sup> and Kaufman et al.<sup>31</sup> U 87 MG cells (MTX resistant and sensitive) were plated into 24-well plates and were allowed to adhere for 24 h. Later, they were incubated with

(28) Dhanikula, R.; Hildgen, P. *In vitro* evaluation of polyether-co-polyester dendrimers for delivery across the blood brain barrier. *Biomacromolecules* (Submitted).

(29) Alt, F. W.; Kellems, R. E.; Schimke, R. T. Synthesis and degradation of folate reductase in sensitive and methotrexate-resistant lines of S-180 cells. *J. Biol. Chem.* **1976**, *251*, 3063–3074.

(30) Gapski, G. R.; Whiteley, J. M.; Rader, J. I.; Cramer, P. L.; Henderson, G. B.; Neef, V.; Huennekens, F. M. Synthesis of a fluorescent derivative of amethopterin. *J. Med. Chem.* **1975**, *18*, 526–528.

(31) Kaufman, R. J.; Bertino, J. R.; Schimke, R. T. Quantitation of dihydrofolate reductase in individual parental and methotrexate-resistant murine cells. Use of a fluorescence activated cell sorter. *J. Biol. Chem.* **1978**, *253*, 5852–5860.

medium containing 30  $\mu\text{M}$  MTX-FITC for 10 h at 37 °C. After incubation cells were washed four times with HBSS and lysed with 200  $\mu\text{L}$  of 0.5% Triton-X containing 0.1 N NaOH. MTX-FITC concentrations in cell lysates were determined by measuring fluorescence ( $\lambda_{\text{ex}}$  504 nm and  $\lambda_{\text{em}}$  538 nm) using a Safire plate reader (Tecan Austria GmbH, Salzburg, Austria). Standard curve generated using lysed cells and MTX-FITC was used for the quantification of fluorescence in the experiments. Protein content of each well was estimated using micro BCA protein assay reagent.

**2.2.8. Antiproliferative Activity of Dendrimers against Glioma Cells.** Human glioma cell lines, U 87 MG and U 343 MGa, were cultured in DMEM supplemented with 10% FBS, 1% nonessential amino acids, and penicillin/streptomycin at 37 °C in a 5% CO<sub>2</sub> atmosphere. MTX-resistant U 87 MG cells were cultured as mentioned in the previous section. Cells (passage 15–20) were seeded at the concentration of  $1 \times 10^4$  cells/mL (100  $\mu\text{L}$ /well) in 96-well cell culture plates and were allowed to adhere to the wells for 24 h. Cellular growth inhibition was evaluated by MTT assay. Dendrimers loaded with MTX (2 to 1000  $\mu\text{M}$ , in HBSS) were added to the cells and incubated for 72 h. Later, 10  $\mu\text{L}$  of 5 mg/mL of MTT solution was added to each well, followed by incubation at 37 °C for 4 h. Formazan crystals produced by the cells were dissolved in 100  $\mu\text{L}$  of MTT solubilization solution. Absorbance was measured at 570 nm using Safire plate reader (Tecan Austria GmbH, Salzburg, Austria).

**2.2.9. Transport of Dendrimers and MTX across BBB.** Coculture of bEnd.3 (ATCC, Rockville, MD) and U373 MG cells was used as the model for BBB.<sup>28,32,33</sup> bEnd.3 and U373 MG cells were seeded onto polycarbonate Transwell inserts at the density of  $5 \times 10^5$  cells/mL and  $2 \times 10^5$  cells/mL, and confluent monolayers (9–10 days) were used for the transport studies.<sup>28</sup> Permeability was determined in the apical to basolateral direction using HBSS as a transport medium. Rhodamine labeled dendrimers or MTX loaded dendrimers were placed in the donor compartment and plates were incubated in a humidified, CO<sub>2</sub> atmosphere at 37 °C. Samples were collected from the receiver compartment at predetermined time points. They were analyzed for rhodamine-labeled dendrimer using fluorescence plate reader ( $\lambda_{\text{ex}}$  550 nm and  $\lambda_{\text{em}}$  625 nm). MTX was analyzed by HPLC using C-18 column, mobile phase consisting of methanol, 10 mM phosphoric acid, and 10 mM KH<sub>2</sub>PO<sub>4</sub> (26:16:58 v/v, pH 4.5) at a flow rate of 0.9 mL/min and wavelength of 290 nm using a Waters 717 system equipped with Waters<sup>TM</sup> 486 tunable absorbance detector (Waters Corporation, Mil-

ford, MA). The effect of dendrimers on BBB integrity was investigated by monitoring transendothelial electrical resistance (TEER) throughout the experiment.

**2.2.10. Avascular Human Glioma Tumor Spheroids.** Tumor spheroids of U 87 MG and U 343 MGa cells were grown *in vitro* using liquid overlay system.<sup>34,35</sup> Agarose solution was prepared in serum free DMEM (2% w/v) by heating it at 80 °C for 30 min. Each well of cell culture plates was coated with a thin layer (0.3 mL) of this sterilized solution. Tumor cells at the density of  $1 \times 10^5$  cells/mL (in complete medium) were seeded into each well. Subsequently, plates were gently agitated for 5 min on the first day of seeding and tumor spheroids were allowed to grow for 7 days at 37 °C in a humidified atmosphere. Medium of the wells was changed every 2–3 days.

**(a) Growth Inhibition of the Tumor Spheroids.** For evaluating the inhibition of tumor growth, tumor spheroids were incubated with PBS, MTX, or MTX-loaded dendrimers. Samples were prepared in PBS (pH 7.4) and 100  $\mu\text{L}$  sample was added per well to obtain a concentration of 200–400  $\mu\text{M}$ . Growth inhibition was monitored by measuring the size of tumor spheroids using an inverted phase microscope fitted with an ocular micrometer. The major ( $d_{\text{max}}$ ) and minor ( $d_{\text{min}}$ ) diameters of each spheroid were determined and spheroid volume was calculated as mentioned previously<sup>36</sup> by using the following formula:

$$V = \frac{\pi \times d_{\text{max}} \times d_{\text{min}}}{6} \quad (1)$$

**(b) Determination of Cell Viability in the Tumor Spheroids.** Ethidium bromide was used as a fluorescent probe for determining the dead cells in the tumor spheroids after treatment with MTX or MTX-loaded dendrimers. For this purpose, tumor spheroids were incubated with PBS, MTX, or MTX-loaded dendrimers for 7 days. Subsequently, they were incubated with ethidium bromide (50  $\mu\text{g}/\text{mL}$ ) for 20 min at 4 °C. After incubation, they were washed four times with PBS and disintegrated with 0.5% Triton-X containing 0.1 N NaOH. Fluorescence in the cell lysate was measured by using Safire plate reader (Tecan Austria GmbH, Salzburg, Austria). Protein content of tumor spheroids was estimated using micro BCA protein assay reagent.

**(c) Diffusion of Dendrimers into the Tumor Spheroids.** Tumor spheroids were incubated with rhodamine-labeled dendrimers (200  $\mu\text{g}/\text{mL}$ ) for 1, 2, 4, 6, 12, and 24 h. At specified time points, spheroids were washed four times

(32) Omid, Y.; Campbell, L.; Barar, J.; Connell, D.; Akhtar, S.; Gumbleton, M. Evaluation of the immortalised mouse brain capillary endothelial cell line, bEnd3, as an *in vitro* blood-brain barrier model for drug uptake and transport studies. *Brain Res.* **2003**, *990*, 95–112.

(33) Song, L.; Pachter, J. S. Culture of murine brain microvascular endothelial cells that maintain expression and cytoskeletal association of tight junction-associated proteins. *In Vitro Cell Dev. Biol. Anim.* **2003**, *39*, 313–320.

(34) Kobayashi, H.; Man, S.; Graham, C. H.; Kapitain, S. J.; Teicher, B. A.; Kerbel, R. S. Acquired multicellular-mediated resistance to alkylating agents in cancer. *Proc. Natl. Acad. Sci. U.S.A.* **1993**, *90*, 3294–3298.

(35) Rofstad, E. K.; Wahl, A.; Cde, L. D.; Brustad, T. Growth characteristics of human melanoma multicellular spheroids in liquid-overlay culture: comparisons with the parent tumour xenografts. *Cell Tissue Kinet.* **1986**, *19*, 205–216.

(36) Ballangrud, A.; Yang, W.-H.; Dnistrian, A.; Lampen, N.; Sgouros, G. Growth and characterization of LNCap prostate cancer cell spheroids. *Clin. Cancer Res.* **1999**, *5*, 3171s–3176s.

with HBSS, fixed with formaldehyde (10% w/v in PBS) for 30 min, and placed in cavity microscope slides. Confocal laser scanning microscope images were acquired at 10 X using confocal microscope described above. Eight-micrometer-thick optical sections were acquired from the top toward the center of the spheroids approximately 136  $\mu\text{m}$  deep into the spheroid.

### 3. Results

#### 3.1. Conjugation of Glucosamine to the Dendrimers.

Conjugation of glucosamine to the dendrimers was carried out by using disuccinimidyl carbonate so that the amino group of the glucosamine was selectively activated to form succinimidyl derivative. This would in turn result in glucosamine conjugated to the dendrimers by a carbamate linkage. Characterization of the products by FTIR and  $^1\text{H}$  NMR (Figure 1s, Supporting Information) proved the successful synthesis. The number of glucosamine molecules attached to each dendrimer was also determined by  $^1\text{H}$  NMR spectroscopy. Three glucosamine molecules per dendrimer were found to be conjugated in den-1-(G2)-400-Glu, while den-2-(G2)-400-Glu had five glucosamine molecules conjugated per dendrimer.

#### 3.2. MTX Loading in the Dendrimers.

MTX loading in the dendrimers of den-1-series ranged between 17.2 and 21.9% w/w, while in that of den-2-series ranged between 20.3 and 24.5% w/w (Table 1). Dendrimers with PEO 400 Da in the interior cavity encapsulated a higher amount of MTX as compared to dendrimers with PEO 300 and 200 Da in both den-1-series and den-2-series, with MTX loading of 21.9% w/w in den-1-(G2)-400 and 24.5% w/w in den-2-(G2)-400. MTX loading in glucosylated dendrimers was lower than corresponding nonglucosylated dendrimers, with den-1-(G2)-400-Glu and den-2-(G2)-400-Glu encapsulating 19.4% w/w and 20.8% w/w of MTX, respectively.

#### 3.3. Internalization of Dendrimers by the Glioma Cells.

U 87 MG and U343 MGa cells endocytosed approximately 76 and 347  $\mu\text{g}/\text{mg}$  of protein of rhodamine-labeled den-1-(G2)-400 in 6 h (Figure 1a). For both cell lines, the amount of dendrimers internalized by the cells increased with time until 6 h but decreased at 12 h (Figure 1). The extent of internalization of dendrimers was three to five times greater in U 343 MGa cells than in U 87 MG cells. The reason for the higher endocytosis of dendrimers in U343 MGa cells is not yet understood. Conjugation of glucosamine significantly increased the endocytosis of the dendrimer to 603  $\mu\text{g}/\text{mg}$  of protein, i.e., by 8-fold in U87 MG and to 672  $\mu\text{g}/\text{mg}$  of protein, i.e., by approximately 2-fold in U 343 MGa cells (Figure 1b). Confocal laser scanning microscopy images of the human glioma cells incubated with rhodamine-labeled dendrimers also showed that dendrimers internalized in high amount within 4 h of incubation and localized mainly in the cytoplasm (Figure 2).

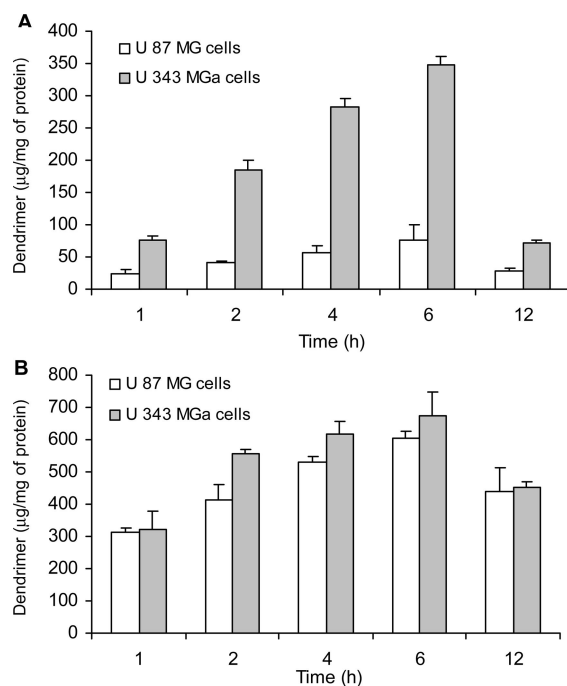


**Figure 1.** Extent of internalization of rhodamine-labeled (A) den-1-(G2)-400 and (B) den-1-(G2)-Glu in the human glioma cells. Data are mean values ( $n = 6 + \text{SD}$ ).

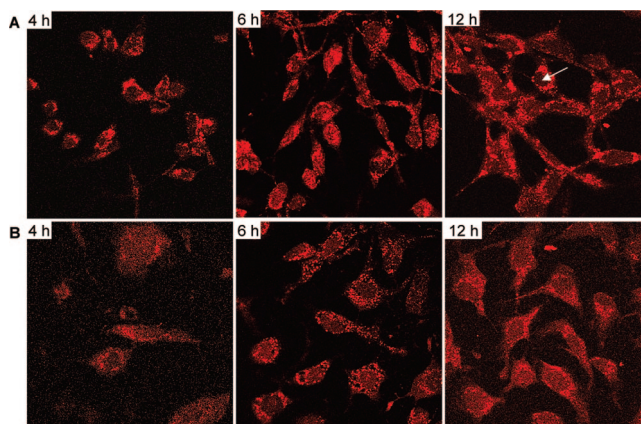


**Figure 2.** Confocal microscope images of U 343 MGa cells incubated with (A) rhodamine-labeled den-1-(G2)-400 and (B) rhodamine-labeled den-1-(G2)-Glu. Images were acquired at 100 $\times$ . White arrow indicates nuclei of the cell.

#### 3.4. Characterization of MTX-Resistant U87 Cells.

Microscopic examination of MTX-resistant cells showed marked differences in the morphological features; primarily, MTX-resistant U 87 MG cells were larger, with larger nuclei and cellular granules in the cytoplasm (Figure 2s, Supporting Information). The DHFR activity in the cell extracts of MTX-resistant U 87 MG cells was found to be  $0.89 \pm 0.22 \mu\text{M}/\text{min}/\text{mg}$  of protein, while in MTX-sensitive cells it was  $0.39 \pm 0.19 \mu\text{M}/\text{min}/\text{mg}$  of protein. The difference in the activity of DHFR proved that MTX-resistant cells were successfully developed.<sup>29</sup> It also indicated that MTX-sensitive U 87 MG cells had a higher ability to convert folic acid to dihydrofolic acid, and thus, lower activity of DHFR enzyme in the cells

**Table 2.** IC<sub>50</sub> Values of MTX and MTX-Loaded Dendrimers against Different Human Glioma Cell Lines<sup>a</sup>

sample	U 87 MG cells (μM)	U 343 MGa cells (μM)	MTX-resistant U87 MG cells (μM)
MTX	2.14 ± 0.34	2.79 ± 0.64	85.95 ± 3.52
Den-1-(G2)-200	1.28 ± 0.08**	0.62 ± 0.16***	
Den-1-(G2)-300	1.91 ± 0.25**	0.59 ± 0.07***	
Den-1-(G2)-400	1.93 ± 0.44**	0.70 ± 0.11***	5.22 ± 0.86***
Den-1-(G2)-400-Glu	0.43 ± 0.05***	0.39 ± 0.13***	1.17 ± 0.41***
Den-2-(G2)-200	1.42 ± 0.81**	1.30 ± 0.18**	
Den-2-(G2)-300	1.41 ± 0.26**	1.35 ± 0.19**	
Den-2-(G2)-400	1.22 ± 0.36**	0.90 ± 0.22***	3.88 ± 0.61***
Den-2-(G2)-400-Glu	0.35 ± 0.08***	0.42 ± 0.15***	2.02 ± 0.52***

<sup>a</sup> Data are mean ± SD (*n* = 5–6). Statistical analysis was performed using t-test and post-hoc Man–Whitney Rank Sum test (\* *p* < 0.05), \*\* *p* < 0.001, and \*\*\* *p* < 0.005.

was one of the sources of MTX resistance. MTX-resistant cells accumulated MTX-FITC approximately two times higher than MTX-sensitive U 87 MG cells (Figure 3s, Supporting Information), suggesting the presence of higher levels of DHFR in MTX-resistant cell lines.<sup>31</sup>

**3.5. Antiproliferative Activity of Dendrimers against Glioma Cells.** The cytotoxicity of the dendrimers alone on the brain endothelial cells<sup>28</sup> and U87 MG cells were evaluated to ascertain their safety. None of the dendrimers showed significant cytotoxicity against bEnd.3 and U 87 MG cells at concentrations of 0.01–5 mg/mL (Figure 4s, Supporting Information). Inhibition in the growth of two glioma cell lines was tested in the present study to evaluate their potential in different types of gliomas. IC<sub>50</sub> values of MTX toward U 87 MG and U 343 MGa cells were 2.14 and 2.79 μM, respectively (Table 2). In both the cell lines, MTX loaded in dendrimers had 1.5–5 times lower IC<sub>50</sub> value than the free MTX. Against MTX resistant U 87 MG cells, MTX encapsulated in the dendrimers had IC<sub>50</sub> values 9 to 15 times lower (1.17 to 5.22 μM) than that of the free MTX (85.95 μM). The conjugation of glucosamine to dendrimers further reduced the IC<sub>50</sub> of MTX, but the extent of reduction was dependent on the cell line. MTX loaded dendrimer-glucosamine conjugates were 3.5 to 4.5 times more potent than dendrimers alone toward U 87 MG cells with IC<sub>50</sub> values of 0.35 ± 0.08 and 0.43 ± 0.05 μM and 2 times more toxic toward U 343 MGa cells with IC<sub>50</sub> values of 0.39 ± 0.13 and 0.42 ± 0.15 μM (Table 2). This indicates that there is variation in the extent of uptake of glucosylated dendrimers and, hence, expression of glucose transporters in these cell lines. Even in the MTX-resistant cell lines, glucosylated dendrimers were two to five times more effective in inhibiting the cell growth (Table 2). The influence of increasing the number of glucosamine units from 3 (den-1-(G2)-400-Glu) to 5 (den-2-(G2)-400-Glu) on potency was not apparent in the IC<sub>50</sub> values.

**3.6. Transport of Dendrimers and MTX across the BBB.** The cumulative permeation of rhodamine-labeled dendrimers across the BBB model was highest for den-1-(G2)-400-Glu (345 μg) followed by den-2-(G2)-400-Glu (242 μg), den-2-(G2)-400 (204 μg), and den-1-(G2)-400 (102 μg) (Figure 3). No significant reduction in the TEER was

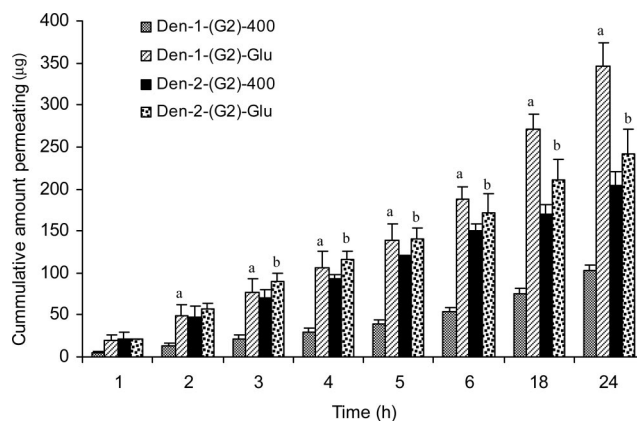


**Figure 3.** Transport of rhodamine-labeled dendrimers across the BBB model (coculture of bEnd.3 and U373 MG cells) at 37 °C. Data are mean values (*n* = 4 + SD). Key: (a) statistically significant difference between den-1-(G2)-400 and den-1-(G2)-Glu, den-2-(G2)-400 and den-2-(G2)-Glu (*p* < 0.001, *t* test and posthoc Man–Whitney rank sum test) and (b) between den-2-(G2)-400 and den-2-(G2)-Glu after 2 h (*p* < 0.05, *t* test and posthoc Man–Whitney rank sum test).

observed throughout the study (Figure 5s, Supporting Information), indicating that dendrimers were able to cross BBB without disruption of its barrier properties. Glucosylated dendrimers were able to permeate across BBB more than dendrimers alone. In the case of den-1-(G2)-400-Glu, the extent of permeation was 3.5 times higher than that of den-1-(G2)-400, while in den-2-(G2)-400-Glu it was 1.2 times higher than den-2-(G2)-400 (Figure 3). The permeability of dendrimer with five glucosamine units (den-2-(G2)-400-Glu) was marginally higher than one with three units (den-1-(G2)-400-Glu), suggesting that three glucosamine units could be ideal for enhanced delivery across the BBB. Encapsulation of MTX in the dendrimers increased the amount of MTX transported across the BBB by three–four-folds. Approximately 0.11 mM MTX was transported across BBB over a period of 12 h (Figure 4). This was increased to 0.37 mM by den-1-(G2)-400, to 0.73 mM by den-1-(G2)-400-Glu, to 0.58 mM by den-2-(G2)-400, and to 0.69 mM by den-2-(G2)-400-Glu (Figure 4). It was also seen that conjugation of three glucosamine molecules to the dendrimers (den-1-(G2)-400-

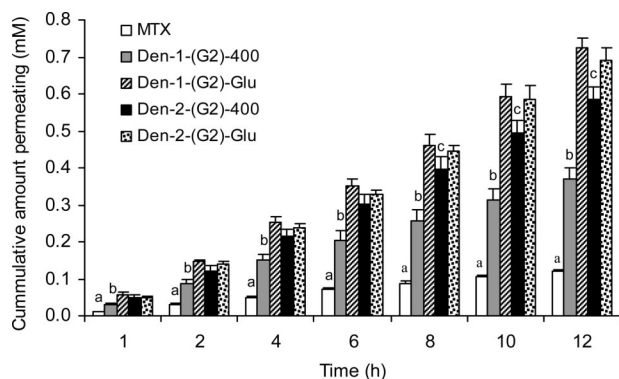


**Figure 4.** Cumulative amount of MTX permeating across the BBB model at 37 °C. MTX or MTX-loaded dendrimers were placed in the donor compartment of Transwell inserts, and the amount of MTX permeating into the receiver compartment was analyzed by HPLC. Data are mean values ( $n = 4 + SD$ ). Key: (a) statistically significant difference between free MTX and all dendrimers ( $p < 0.0001$ ,  $t$  test and posthoc Man–Whitney Rank Sum test), (b) between den-1-(G2)-400 and den-1-(G2)-Glu, den-2-(G2)-400, den-2-(G2)-Glu ( $p < 0.001$ ,  $t$  test and posthoc Man–Whitney rank sum test), and (c) between den-2-(G2)-400 and den-2-(G2)-Glu after 8 h ( $p < 0.05$ ,  $t$  test and posthoc Man–Whitney rank sum test).

Glu) elevated the amount of MTX permeating across the BBB by approximately 2-folds. However, the presence of 5 glucosamine units per dendrimer in den-2-(G2)-400-Glu only marginally increased the amount of MTX available across the BBB, primarily due to greater hydrodynamic size of the corresponding dendrimer (Table 1).

**3.7. Interaction with Avascular Human Glioma Tumor Spheroids.** Confocal laser scanning microscopic imaging of the tumor spheroids showed that in the first 4 h of incubation dendrimers were present only in the periphery; however, the extent of diffusion was greater for the dendrimer with glucosamine ligand (Figure 5). Within 6 h of incubation, glucosylated dendrimer were able to distribute through out the tumor spheroids, while dendrimers without ligand had taken 12 h for the complete distribution (Figure 5). More importantly, it was also seen that the extent of distribution was much higher in glucosamine-conjugated dendrimers.

The influence of various treatments on the growth of tumor spheroids was also studied. It was observed that tumor spheroids continued to grow in size and volume in the absence of any drug (Figure 6b). Free MTX was able to inhibit the growth of tumor spheroids for a few days but produced only marginal reduction in their volume (Figure 6c); on the other hand, MTX-loaded dendrimers produced considerable reduction in the size and volume (Figure 6d,e). The extent of reduction in the tumor volume was different for U 87 MG and U 343 MGa tumor spheroids. In U 87 MG tumor spheroids, tumor spheroid volume was 79%, 75%, 66%, and 65% of the control after 7 days at 0.2 mM MTX and 70%, 69%, 63%, and 71% at 0.4 mM MTX for den-1-(G2)-400, den-1-(G2)-400-Glu, den-2-(G2)-400, and den-2-

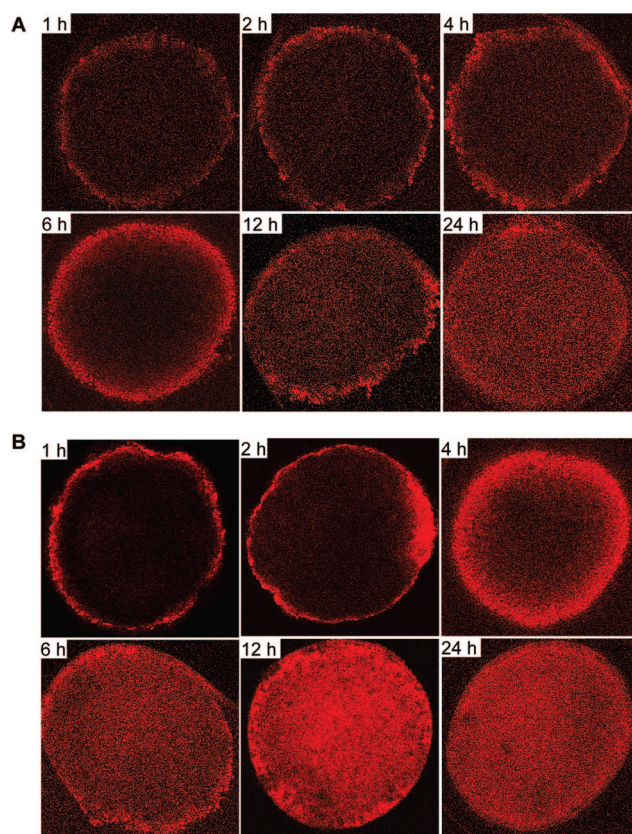


**Figure 5.** Confocal microscope images of U 87 MG tumor spheroids incubated with (A) rhodamine-labeled den-1-(G2)-400 and (B) rhodamine-labeled den-1-(G2)-Glu as a function of time. Images were acquired at 10 $\times$ .

(G2)-400-Glu, respectively (Figure 7). Reduction in the size of tumor spheroids was higher in the case of U 343 MGa tumors spheroids; at 0.2 mM MTX, tumor spheroid volume was 46%, 49%, and 43% of the control after 7 days of incubation, while at 0.4 mM it was 31%, 35%, and 33% for den-1-(G2)-400-Glu, den-2-(G2)-400, and den-2-(G2)-400-Glu, respectively (Figure 7). In both the tumor spheroids, an increase in concentration of MTX increased the activity for all dendrimers except in den-2-(G2)-400-Glu, perhaps due to aggregation at high concentration which reduced uptake by the tumor spheroids. Concentration of ethidium bromide (stains DNA of dead cells) in the tumor spheroids treated with MTX-loaded dendrimer was 13.54  $\mu\text{g}/\text{mg}$  of the protein, while in the control and in those treated with free MTX it was 3.77 and 5.45  $\mu\text{g}/\text{mg}$  of the protein, respectively (Figure 8). In the tumor spheroids treated with glucosylated dendrimer loaded with MTX, ethidium bromide concentration was 18.49  $\mu\text{g}/\text{mg}$  of protein. This clearly indicates that PEPE dendrimers induce a statistically significant increase in cell death as compared to the free MTX ( $p < 0.01$ , one-way ANOVA, post hoc Student–Newman–Keuls test) and also that glucosylation further enhanced this effect ( $p < 0.01$ , one-way ANOVA, post hoc Student–Newman–Keuls test).



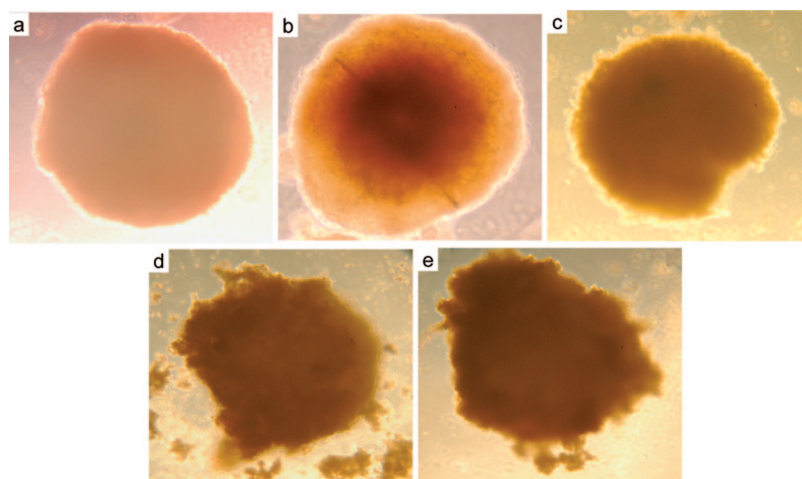


**Figure 6.** Representative micrographs of U 87 MG tumor spheroids (a) before treatment and 4 days after treatment with (b) PBS, (c) MTX (0.4 mM), (d) den-2-(G2)-400 loaded with MTX (0.4 mM), and (e) den-1-(G2)-Glu loaded with MTX (0.4 mM). Images were acquired using 10× objective.

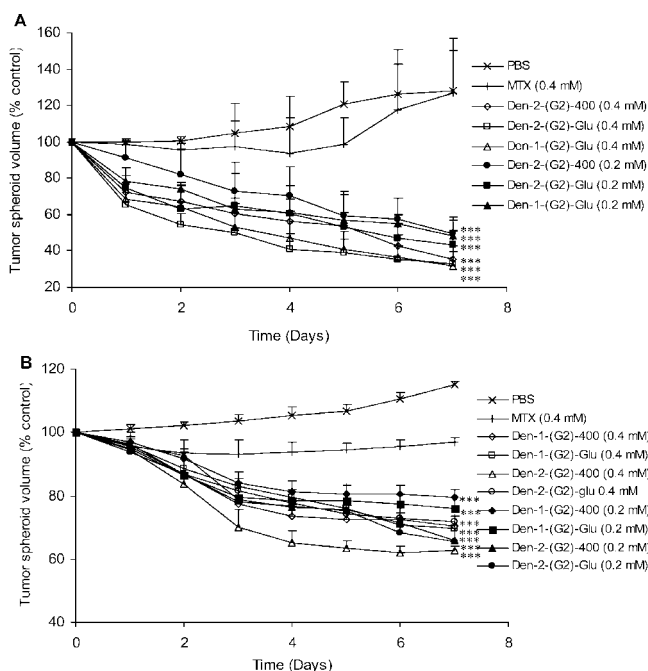


**Figure 7.** Inhibition in the growth of (A) U 343 MGa (B) U 87 MG tumor spheroids on treatment with MTX or MTX-loaded dendrimers. The diameter of tumor spheroids was measured using a microscope fitted with an ocular micrometer, and the volume of the spheroids was calculated. Data are mean values ( $n = 4 + SD$ ). \*\*\*Statistically significant difference with respect to MTX ( $p < 0.005$ , one-way RM ANOVA, post hoc Student–Newman–Keuls test).

#### 4. Discussion

The basic GLUT is reported to play a major role in glucose uptake by the tumor cells. Though glucose transporters are expressed in all of the tissues, the major difference between normal and cancerous cells is the presence of facilitative glucose transporter (GLUT) genes in the latter.<sup>16</sup> Glucose-conjugated niosomes have been reported to have higher tumor-to-muscle accumulation in the glioma xenografts;<sup>11</sup>

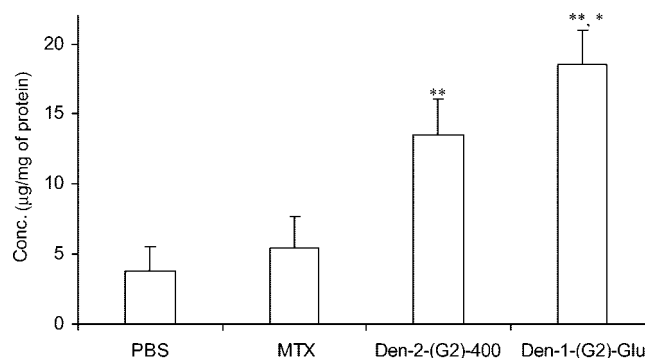


**Figure 8.** Accumulation of ethidium bromide in U 87 MG tumor spheroids subjected to different treatments. Ethidium bromide stains the DNA of dead cells, and thus, its concentration relates to dead cell population. Data are mean values ( $n = 4 + SD$ ). \*\*Statistically significant difference with respect to PBS and MTX ( $p < 0.05$ , one-way ANOVA, post hoc Student–Newman–Keuls test). \*Statistically significant difference with respect to den-2-(G2)-Glu ( $p < 0.01$ , one-way ANOVA, post hoc Student–Newman–Keuls test). Note: Den-2-(G2)-400 and den-2-(G2)-400 were selected because they produced greater reduction in U 87 MG tumor spheroid size at 0.4 mM.

Kim et al.<sup>37</sup> have also demonstrated that glucose-conjugated PEI enhance gene delivery to the lung cancer. Additionally, targeting GLUT-1 can be potentially employed for enhanced delivery of the carriers across BBB.<sup>9</sup> Dendrimers conjugated to glucose are small and mimic glucose; in fact, that they have been reported to compete with glucose in glucose assay.<sup>38</sup> Thus, they can be taken up by the GLUT on BBB

- (37) Kim, H. W.; Park, I. K.; Cho, C. S.; Lee, K. H.; Beck, G. R. J.; Colburn, N. H.; Cho, M. H. Aerosol delivery of glucosylated polyethylenimine/phosphatase and tnsin homologue deleted on chromosome 10 complex suppresses Akt downstream pathways in the lung of K-ras null mice. *Cancer Res.* **2004**, *64*, 7971–7976.
- (38) Beier, H.; Ibey, B.; Pishko, M.; Cote, G. Use of glycosylated dendrimer macromolecules to fluorescently monitor glucose concentration. *Proc. SPIE* **2007**, *6445*, 644–504.

as well as tumor cells. Due to these advantages offered by GLUT targeting, glucosamine conjugates of dendrimers were synthesized in this study. D-Glucosamine, 2-amino-2-deoxy-D-glucose, was chosen as a ligand because it is reported that modification at 2 position of the glucose ring does not alter its interaction with GLUT; additionally, presence of an amino group would allow easy and reproducible conjugation. The influence of glucosamine ligand on the targetability of the dendrimers was determined by studying the extent of internalization of dendrimers by the glioma cells. It was found that glucosylated dendrimers had 2–8-fold higher levels in all the glioma cells (U 87 MG and U343 MGa) in 6 h (Figure 1), suggesting that glucosamine ligand significantly enhanced the internalization of the dendrimers by the glioma cells. Confocal microscopy showed that dendrimers were present throughout the cytoplasm within 4 h (Figure 2). The pattern of distribution of dendrimers in the cells was not found to be influenced by the conjugation of glucosamine to the dendrimers. However, greater fluorescence seen in the nucleus of cells treated with den-1-(G2)-400-Glu suggested their entry into the nucleus.

PEPE dendrimers were able to encapsulate a high amount of MTX (20.3–24.5% w/w, Table 1) as compared to PEG-grafted PAMAM dendrimers which could encapsulate 10–13 mol of MTX/mol of dendrimer.<sup>39</sup> The amount of MTX loaded in the dendrimers increased with the molecular weight of PEO in the interior in the both series due to augmentation in the size of interior voids with increase in the molecular weight of PEO.<sup>27</sup> Conjugation of glucosamine to the dendrimers was seen to decrease the loading for both the den-1-series and den-2-series (Table 1). This could happen due to the hindered diffusion of the MTX molecules into the interior of the dendrimers because of the steric hindrance offered by the glucosamine units at the surface or due to the bending of glucosamine units into the dendritic structure. Nevertheless, even in the presence of glucosamine units the drug loading was significantly high.

Recently, dendrimers have been utilized for the delivery of various chemotherapeutic agents including MTX. However, in most of these studies, MTX was conjugated to the terminal groups of the dendrimers. These conjugates have failed to provide increase in the therapeutic benefit; for instance, Wu et al.<sup>40</sup> reported that MTX conjugated to PAMAM dendrimers did not show any improvement in the potency either due to reduced binding of the conjugate to DHFR or due to low cleavage of MTX from the conjugate.

In another study, Patri et al.<sup>41</sup> reported that the PAMAM, folic acid, and MTX conjugate had higher IC<sub>50</sub> than free MTX. They also reported that MTX loading in PAMAM dendrimers did not increase its potency.<sup>41</sup> This was attributed to the fast release of MTX from PAMAM dendrimers. However, in the present study, MTX-loaded dendrimers were more efficacious than free MTX (Table 2). Glucosylation of the dendrimers further improved the potency of these MTX-loaded dendrimers against the glioma cells by approximately 2–4.5-fold (Table 2). The higher potency of glucosylated dendrimers can be correlated to their higher cellular uptake as compared to nonglucosylated dendrimers by the glioma cells (Figure 1). Further, dendrimers were able to notably overcome the MTX resistance and reduce the IC<sub>50</sub> by approximately 9–15 times (Table 2). The ability of these dendrimers to improve the potency of MTX toward the resistant glioma cell lines suggests that drug is released from the dendrimers after entering the cells. And that dendrimers enter the cells by mechanism different from that of the uptake of MTX. MTX is reported to be taken up into the mammalian cells by the reduced folate receptors<sup>42</sup> and the loss of the functions of this receptor is a common cause of MTX resistance.<sup>43</sup> Thus, in addition to lower DHFR activity, lower uptake of MTX by U 87 MG cells is also one of the factors in the resistance of these cells to MTX. From these results, it is evident that PEPE dendrimers are able to deliver high payload of MTX intracellularly.

The low permeability of delivery systems across BBB is the major limitation in the delivery of drugs to the brain. Therefore, the permeability of dendrimers across BBB was evaluated in this study. Recently, various *in vitro* BBB model have emerged as a valuable method to investigate permeability of drug and delivery systems across BBB in early development stages. These models retain many features of BBB like presence of tight junction elements like ZO-1, occludin, claudin-1 and various transporters like GLUT-1, OAT1, amino acid carriers, P-gp.<sup>32,33</sup> A strong correlation between the permeability of various drug across BBB models and human brain concentration is reported.<sup>44,45</sup> Thus, the permeability of dendrimers and glucosylated dendrimers across *in vitro* BBB model was determined in the present study. Dendrimers were able to permeate the BBB and reach

- (39) Kojima, C.; Kono, K.; Maruyama, K.; Takagishi, T. Synthesis of polyamidoamine dendrimers having poly(ethylene glycol) grafts and their ability to encapsulate anticancer drugs. *Bioconjugate Chem.* **2000**, *11*, 910–917.
- (40) Wu, G.; Barth, R.; Yang, W.; Kawabata, S.; Zhang, L.; Green-Church, K. Targeted delivery of methotrexate to epidermal growth factor receptor-positive brain tumors by means of cetuximab (IMC-C225) dendrimer bioconjugates. *Mol. Cancer Ther.* **2006**, *5*, 52–59.

- (41) Patri, A.; Kukowska-Latallo, J.; Baker, J. J. Targeted drug delivery with dendrimers: comparison of the release kinetics of covalently conjugated drug and non-covalent drug inclusion complex. *Adv. Drug Deliv. Rev.* **2005**, *57*, 2203–2214.
- (42) Matherly, L.; Goldman, D. Membrane transport of folates. *Vitam. Horm.* **2003**, *66*, 403–456.
- (43) Zhao, R.; Goldman, D. Resistance to antifolates. *Oncogene* **2003**, *22*, 7431–7457.
- (44) Dehouck, M.-P.; Jolliet-Riant, P.; Brée, F.; Fruchar, J.-C.; Cecchelli, R.; Tillement, J.-P. Drug transfer across the Blood-Brain Barrier: Correlation between *in vitro* and *in vivo* models. *J. Neurochem.* **1992**, *58*, 1790–1797.
- (45) Lundquist, S.; Renftel, M.; Brillault, J.; Fenart, L.; Cecchelli, R.; Dehouck, M.-P. Prediction of drug transport through the Blood-Brain Barrier *in vivo*: A comparison between two *in vitro* cell models. *Pharm. Res.* **2002**, *19*, 976–981.

the receiver compartment in high amounts (Figure 3). In the previous study,<sup>28</sup> we established that rhodamine-labeled PEPE dendrimers cross the BBB model and not merely rhodamine crosses into the receiver compartment. Notably, the extent of permeation of den-2-(G2)-400 was 2 times higher than that of den-1-(G2)-400. It is speculated that this higher permeation of the former across BBB was due to higher number of PEG chains present on the surface.<sup>27</sup> Den-1-(G2)-400-Glu had 3.5 times greater permeability in comparison with den-1-(G2)-400, while Den-2-(G2)-400-Glu had moderately higher permeation (1.2 folds) than den-2-(G2)-400 (Figure 3). It is hypothesized that moderate augmentation in the permeability of den-2-(G2)-400-Glu as compared to den-2-(G2)-400 is because of the larger size of the glucosylated dendrimer due to the presence of 5 glucosamine moiety which reduces its endocytosis (Table 1). Nonetheless, higher permeability of glucosylated dendrimers suggests that glucosamine serves to increase the permeability of dendrimers across the BBB. The effect of higher permeability of glucosylated dendrimers were reflected in the amount MTX delivered by these dendrimers across BBB (Figure 4). Encapsulation of MTX in den-1-(G2)-400 and den-2-(G2)-400 increased the amount of MTX available across BBB 4 and 6 times, respectively (Figure 4). Glucosylation of den-1-(G2)-400 and den-2-(G2)-400 increased the availability of MTX across BBB by 2-folds in den-1-(G2)-400-Glu, but only by approximately 1-fold in den-2-(G2)-400-Glu (Figure 4). A lower increment in the MTX availability by the latter can be explained by its lower permeability across the BBB (Figure 3). Interestingly, den-1-(G2)-400-Glu transported 7 times higher amount of MTX as compared to the free MTX. Thus, conjugation of three glucosamine molecules per dendrimer seems to be ideal for enhancing the permeability of PEPE dendrimers across the BBB. Accordingly, these PEPE dendrimers can be used for the delivery of a higher amount of MTX across BBB and the conjugation to glucosamine can further augment it.

Due to the poor permeation of delivery systems into the hypoxic and necrotic tumor regions distant from the vascular bed, the amount of drug accessing inside the solid tumors is low.<sup>20,22,46</sup> As a consequence, the overall therapeutic effect of chemotherapeutic agents is restricted, leading to the relapse of cancer. These limitations of delivery systems are particularly dangerous in malignant gliomas which are one of the most refractory tumors.<sup>47,48</sup> It is postulated that enhancement in the ability of the delivery system to penetrate deeper into the tumor tissues can significantly reduce the tumor regrowth and augment the therapeutic benefit of the treatment. It has been reported that tumor spheroids generated by liquid overlay technique are not only aggregates of cells in close contact but contain an organized extracellular matrix consisting of fibronectin, laminin, collagen, and GAG, suggestive of the extracellular matrix of tumors *in vivo*.<sup>49,50</sup> Therefore, interstitial penetration and diffusion of dendrimers into

avascular regions of the solid tumors was evaluated using tumor spheroids as a model. Rhodamine-labeled dendrimers were able to reach the central necrotic region of the tumor spheroids within 12 h of incubation (Figure 5). Glucosylation was found to enhance the rate and extent of diffusion of the dendrimers in the tumor spheroids (Figure 5). This is because the central regions of the solid tumors are hypoxic and demonstrate a hypoxia related increase in the glucose transport.<sup>10,51</sup> Thus, greater demand of glucose in the hypoxic regions of the tumors drives the faster and enhanced distribution of glucosylated dendrimers in the tumors spheroids. This finding suggests these PEPE dendrimers would probably reach the avascular regions of the tumors within 150–200  $\mu\text{m}$  and thus would provide more effective control of the tumor growth. Further, evaluation of the ability of these dendrimers to reach avascular regions of tumors would be tested in *in vivo* brain tumor models.

MTX-loaded dendrimers were able to considerably reduce the size of tumor spheroids during 7 days of the study (Figures 6 and 7). U 87 MG tumor spheroids volumes were reduced to 63–79% of the control, while U 343 MGa tumor spheroids volume was decreased to 31–49% of the control (Figure 7). The potency of the MTX loaded dendrimers was always higher than that of the free MTX (significant difference,  $p < 0.005$ , one way RM ANOVA). However, the therapeutic gain obtained from glucosylated dendrimers on tumor spheroids was different depending on the type of glioma cells. In both of the tumor spheroids, den-1-(G2)-400-Glu was more effective than den-1-(G2)-400, while den-2-(G2)-400-Glu was either more effective than or as effective as den-2-(G2)-400 at the tested concentrations (Figure 7). This could be due to the fact that den-2-(G2)-400-Glu has greater size than den-1-(G2)-400-Glu and hence lower penetration in the tumor spheroids (Table 1). The concentration of ethidium bromide in the lysate of tumor spheroids treated with MTX loaded nonglucosylated and glucosylated dendrimers dendrimer was significantly higher than in those treated with free MTX ( $p < 0.01$ , one-way ANOVA, post hoc Student–Newman–Keuls test) (Figure 8). Ethidium bromide concentration is related to the population of dead

(46) Minchinton, A.; Tannock, I. Drug penetration in solid tumours. *Nat. Rev. Cancer* **2006**, *6*, 583–592.

(47) Desjardins, A.; Rich, J.; Quinn, J.; Vredenburgh, J.; Gururangan, S.; Sathornsumetee, S.; Reardon, D.; Friedman, A.; Bigner, D.; Friedman, H. Chemotherapy and novel therapeutic approaches in malignant glioma. *Front Biosci.* **2005**, *10*, 2645–2668.

(48) Graham, C.; Cloughesy, T. Brain tumor treatment: chemotherapy and other new developments. *Semin. Oncol. Nurs.* **2004**, *20*, 260–272.

(49) Paulus, W.; Huettner, C.; Tonn, J. C. Collagens, integrins and the mesenchymal drift in glioblastomas: a comparison of biopsy specimens, spheroid and early monolayer cultures. *Int. J. Cancer* **1994**, *58*, 841–846.

(50) De Lange Davies, C.; Müller, H.; Hagen, I.; Garseth, M.; Hjelstuen, M. H. Comparison of extracellular matrix in human osteosarcomas and melanomas growing as xenografts, multicellular spheroids, and monolayer cultures. *Anticancer Res.* **1997**, *17*, 4317–4326.

(51) Clavo, A. C.; Brown, R. S.; Wahl, R. L. Fluorodeoxyglucose uptake in human cancer cell lines is increased by hypoxia. *J. Nucl. Med.* **1995**, *36*, 1625–1632.

cells in the sample, thereby suggesting that MTX loading in the dendrimers significantly enhanced the percentage kill of the cells in the tumor spheroids. This is attributed to enhanced entry of dendrimers into tumor spheroids as well as slow release of MTX after loading in these dendrimers.<sup>27</sup> Since, the tumor spheroids mimic the microenvironment of solid tumors, the higher efficacy of MTX loaded dendrimers suggests that they would provide significantly higher therapeutic benefit than MTX.

In a nutshell, this study shows that MTX-loaded PEPE dendrimers are more potent than free MTX as well as effective against MTX-resistant glioma cells. They can deliver MTX across BBB in high amounts and can penetrate into the central necrotic regions of avascular tumor spheroids. Additionally, glucosylation not only increases their potency but also enhances their permeability across the BBB and diffusion into the avascular regions of the tumor tissue. Hence, glucosylated PEPE dendrimers can serve as effective delivery systems for the treatment of gliomas. Further *in vivo* studies to test the proof-of-concept will be carried out in the future. It is speculated that these glucosylated dendrimers

with ability to counteract drug resistance and enhance drug delivery to the central avascular regions of the tumor can serve as a step forward to improving the efficacy of chemotherapy.

**Acknowledgment.** We thank Jean-Michel Rabanel for technical assistance with the confocal laser scanning microscopy experiments. A graduate research scholarship awarded to R.S.D. by Rx & D Health Research Foundation and Canadian Institutes of Health Research (CIHR) is gratefully acknowledged. P.H. thanks the Natural Sciences and Engineering Research Council of Canada (NSERC) for the research funding. This study was partially funded by a NSERC grant to J.-F.B. A.A. is supported by a CNIB-CIHR studentship and J.-F.B. by a Rx & D Health Research Foundation and CIHR Scholar award.

**Supporting Information Available:** Schemes showing the synthesis of the core and dendrimers; NMR spectra. This material is available free of charge via the Internet at <http://pubs.acs.org>.

MP700086J